Macromolecules

pubs.acs.org/Macromolecules Article

Highly Regioselective Ring-Opening Polymerization of an Asymmetric Diester

Yeqi Du, Jinbo Hu, Wenbo Wang, Xinyan Liu, Yanlong Liu, Ranlong Duan,* Xinchao Bian,* and Xuesi Chen

Cite This: *Macromolecules* 2024, 57, 11476−11487 Read Online

ACCESS | Metrics & More | Article Recommendations | Supporting Information

ABSTRACT: Controlling the monomer sequence in hydroxy acid copolymers remains a significant challenge, yet it is essential for fine-tuning the properties of copolyesters. This study presents the regioselective ring-opening polymerization (ROP) of L-3-*tert*-butyl-6-methyl-1,4-dioxane-2,5-dione (L-tBMG), resulting in the synthesis of alternating polylactic acid-*co*-2-*tert*-butylglycolic acid copolymers. The process is facilitated by enantiomerically pure Schiff base aluminum catalysts featuring either a binaphthyl framework or a 2,2-dimethylpropylenediamine and 3,5-dichlorosalicylaldehyde framework. These catalysts promote regioselective ring-opening of the asymmetric cyclic diester specifically at the acyl-oxygen bond of the lactic acid moiety. The molecular chain structure of the resulting polymers was elucidated through heteronuclear multiple bond correlation spectroscopy, while chain regularity was assessed using ^{1}H NMR and quantitative ^{13}C NMR (q-^{13}C NMR). According to the ^{1}H NMR and q-^{13}C NMR test results, the molecular chain regularity is about 0.93. Incorporation of 2-*tert*-butylglycolic acid units led to a glass transition temperature (T_g) of the random copolymer to 65 °C. Notably, the T_g of the isotactic polymer, synthesized via ROP catalyzed by the aforementioned catalysts, was further elevated to 70 °C.

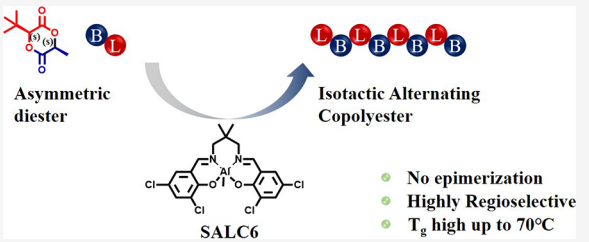

INTRODUCTION

The widespread use of petroleum-based plastics has led to increasingly severe environmental pollution and resource crises.[1−3] Biodegradable polyester materials have emerged as a promising solution to these challenges.[4−9] These materials are partly derived from renewable natural resources, including corn starch, straw, and even household waste, making them highly beneficial for sustainable human development.[10] However, the limited variety of biobased polyesters currently available hinders their broader application, and their performance still requires significant improvement.[11] In addition to developing new polyester monomers, precise control over the molecular chain structure of copolymers has become crucial for enhancing polymer properties. Polymer sequence control-the precise arrangement of monomer units within a polymer chain-represents a critical technique for tuning copolymer properties and developing functional materials.[12−15] Nonetheless, this area of research continues to face substantial challenges.

Alternating copolymers, characterized by the alternate linkage of two distinct structural repeating units, offer a unique chain structure that can impart superior properties to the material. For instance, Guillaume and co-workers reported that the copolymer of allyl and benzyl β-malolactonates exhibits an increased melting temperature (T_m) as the alternating level of repeating units increases.[16] Alternating PLGA is another particularly attractive sequence variant, as it demonstrates distinct degradation properties compared to other microstructures in terms of hydrolysis rates, bulk morphology, and thermal behavior.[17−21] Some alternating copolymers can be produced using a simple one-pot method by mixing two monomers, such as the copolymerization of epoxides and anhydrides.[22−27] However, one-pot copolymerization of two different cyclic ester monomers typically results in random copolymers, and reliable synthetic routes for the alternating copolymerization of different hydroxy acids or lactone monomers remain scarce. Previous studies have shown that alternating copolymers can be synthesized using stepwise methods or multicomponent reaction methods, though these approaches are often hampered by cumbersome control methods and broad molecular weight distributions.[28] In contrast, preforming two hydroxy acids into asymmetric diesters and subsequently conducting ring-opening polymerization (ROP) allows for the synthesis of alternating copolymers with controllable molecular weights and narrow molecular weight distributions.[29,30] Research into the synthesis of strictly alternating hydroxy acid copolymers using this method has yielded promising results (Scheme 1a).[28,29,31−33]

Received: September 20, 2024
Revised: November 28, 2024
Accepted: December 3, 2024
Published: December 9, 2024

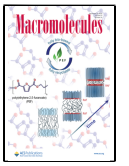

Scheme 1. (a, b) Syntheses of Different Sequence-Controlled Copolyesters via Selective ROP of Asymmetric Diesters

a) Regioselective ROP of asymmetric diesters

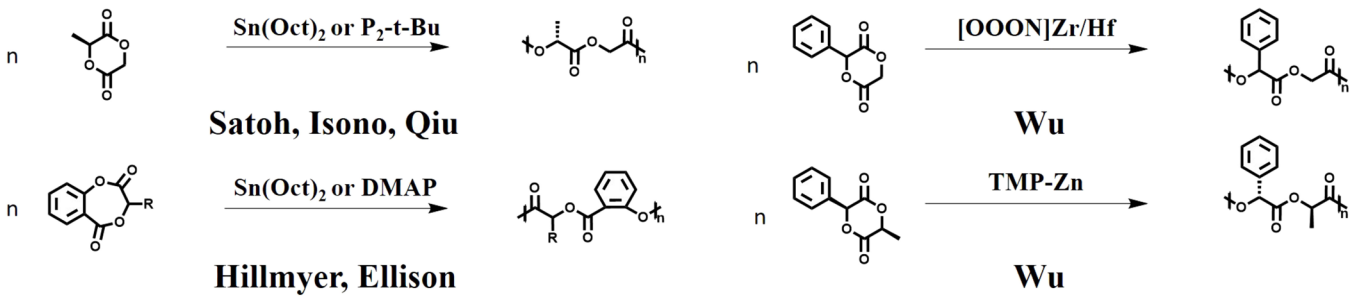

b) This work : regioselective ROP of asymmetric diesters for synthesizing sequence-controlled copolyesters

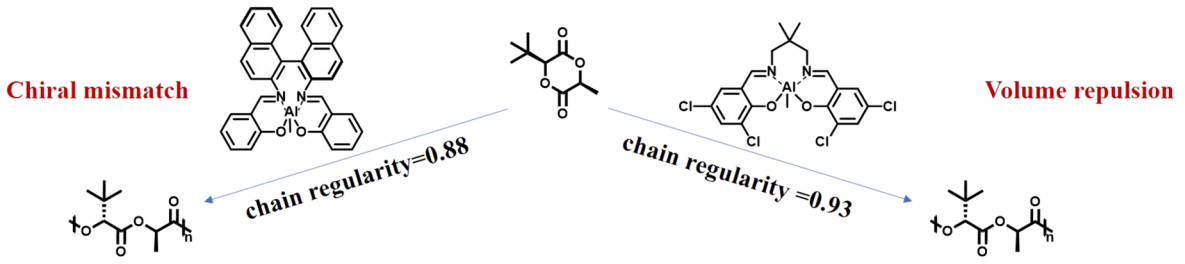

Scheme 2. Synthetic Pathway for the Preparation of Complexes[37,43−47]

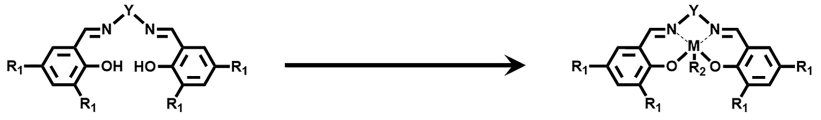

Lignd Complex

Label	Y	R_1	R_2	M
SALC1	(1R,2R)-cyclohexylene	t-Bu	Me	Al
SALC2	1,3-propylenebis	t-Bu	Me	Al
SALC3	2,2-dimethyl-1,3-propylenebis	t-Bu	Me	Al
SALC4	1,3-propylenebis	H	Me	Al
SALC5	2,2-dimethyl-1,3-propylenebis	H	Me	Al
SALC6	2,2-dimethyl-1,3-propylenebis	Cl	Me	Al
$SALC7_R$	(R) -1,1'-binaphthyl-2,2'-diyl	H	Me	Al
$SALC7_S$	(S) -1,1'-binaphthyl-2,2'-diyl	H	Me	Al
SALC8	2,2-dimethyl-1,3-propylenebis	Br	Me	Al
SIFC1	(1R,2R)-cyclohexylene	t-Bu	Cl	Fe
SIFC2	1,3-propylenebis	t-Bu	Cl	Fe

For example, Wu and co-workers achieved highly regioselective polymerization of phenyl-substituted diesters using zirconium and zinc complexes, resulting in alternating polymers with glass transition temperature (T_g) values increased by 5 and 25 °C, respectively, compared to random copolymers.[28,33] These findings underscore the importance of further research into modulating the structural regularity of polymers to improve material properties.

https://doi.org/10.1021/acs.macromol.4c02286
Macromolecules 2024, 57, 11476−11487

Table 1. Polymerization Data of L-tBMG with $Sn(Oct)_2$ and Nonmetal Catalysts[a]

entry	Cat	[M]/[C]/[I]	time (h)	T (°C)	Conv.[b] (%)	$M_{n\ theo}$[c] (kDa)	$M_{n\ GPC}$[d] (kDa)	Đ	chain regularity[e] (%)
1	$Sn(Oct)_2$	100/1/1	2	120	90	16.7	12.3	1.36	
2	TBD	100/1/1	12	−80	90	16.7	13.3	1.26	51
3	MTBD	100/1/1	12	25	67	12.4	6.9	1.08	57
4	MTBD	100/1/1	12	40	84	15.6	11.8	1.32	35
5	DBU	100/1/1	12	40	73	13.6	10.1	1.08	25
6	NHC	100/1/1	12	80	96	17.8	13.2	1.35	53
7[f]	TBD	100/1/1	24	25	95	17.6	15.8	1.12	58
8[f]	MTBD	100/1/1	24	25	52	9.6	8.9	1.09	70
9[f]	DBU	100/1/1	24	25	55	10.2	9.2	1.11	33
10[f]	P1	100/1/1	24	40	73	13.5	11.2	1.21	-
11[f]	NHC	100/1/1	24	40	19	3.5	2.8	1.27	50

[a]All polymerizations were carried out in 4 mL of toluene, [M] = 0.5 mol/L. [b]Measured by ^{1}H NMR. [c]Calculated from the equation molecular weight of L-tBMG × [M]/[I] × conversion. [d]Obtained by GPC in DMF against polystyrene standards. [e]Calculated from the equation chain regularity = (1 − regiodefect) × 100%. The regiodefect was measured by HSQC and HMBC, calculated by q-^{13}C NMR. [f]Added an equivalent amount of thiourea as a cocatalyst.

Polylactic acid, an important biobased polyester, has been widely used in packaging, agriculture, medicine, and other fields.[34−39] Typically, polylactic acid is produced through the ROP of lactide. Atactic and syndiotactic polylactic acids are noncrystalline and have short degradation cycles, making them suitable for packaging materials.[40] Isotactic polylactic acid, with a melting temperature of up to 180 °C, is a promising polymer material. However, its application is limited by its inherently low T_g and low toughness.[41] Previous research has shown that introducing steric hindrance structures of varying sizes into the monomer can effectively adjust the T_g of polylactic acid following ROP.[42] Cyclic diesters are referred to as symmetrical diesters when both sides of the cyclic diester are substituted with the same functional group. Symmetrical diesters can enhance polymer properties through copolymerization with lactide. However, ROP becomes challenging when the substituent group of the symmetrical diester is too large, which restricts the development of new monomer types. Additionally, phenyl substitution of symmetrical diesters increases the Lewis acidity of the hydrogen atom on the methyne, making epimerization more likely during ROP. In contrast, cyclic diesters are termed asymmetric diesters when they are substituted unilaterally or with different functional groups on each side. Asymmetric diesters retain unsubstituted methylene groups or methyne substituted with small functional groups, making their ring-opening polymerization less affected by the substituents and allowing for broader monomer development. However, the asymmetric structure of these diesters leads to variations in the properties of polymers obtained through ROP at different positions. To investigate the relationship between regioselectivity and substituents in ROP, as well as the resulting polymer properties, we preintegrated lactic acid and various hydroxy acids into asymmetric diester monomers. By employing a series of Schiff base complexes to catalyze the ROP, we examined the effects of diester substituent volume and catalyst structure on regioselective ROP. Given the potential impact of monomer sequence on enhancing copolymer properties, this work reports the synthesis of an alternating copolymer of (*S*)-2-hydroxy-2-*tert*-butyl-glycolic acid and lactic acid via highly regioselective ROP of an asymmetric diester monomer, L-3-*tert*-butyl-6-methyl-1,4-dioxane-2,5-dione (L-tBMG) (Scheme 1b), derived from (*S*)-2-hydroxy-2-*tert*-butyl-glycolic acid and lactic acid.

EXPERIMENTAL SECTION

General Considerations. All organic base catalysts were procured from Aldrich Inc. and utilized without further purification. The Salen base complexes (Scheme 2) were synthesized following established protocols as detailed in the literature.[37,43−47] All synthetic procedures and manipulations involving air- and moisture-sensitive materials were conducted under a dry nitrogen atmosphere, either within a glovebox or using standard Schlenk techniques. NMR spectra were acquired using Bruker AV 300M, Bruker AV 500M, and Bruker AV 600 M instruments, with samples dissolved in $CDCl_3$ at 25 °C. Chemical shifts are reported in parts per million (ppm) relative to tetra-methyl-silane (TMS). Gel permeation chromatography (GPC) analyses were performed on a Waters 410GPC system, using DMF as the eluent at a flow rate of 1 mL/min at 35 °C, with molecular weights calibrated against polystyrene (PS) standards. Melting temperature measurements were conducted using a WRS-1B melting point apparatus. Chiral purity was assessed using a Chiral Gas Chromatography (CGC) trace 1300 system. Thermodynamic measurements were carried out using a DSC-Q100 instrument from TA, USA, with all samples tested under a nitrogen flow rate of 50 mL/min and calibration performed with standard indium metal.

Typical Polymerization Procedure. All procedures were carried out in a glovebox, and all ampule bottoms and magnetic stirrers were dried in a high-temperature oven. A representative polymerization procedure is as follows: SALC6 powder (19 mg, 0.04 mmol), a solution of BnOH in toluene (27 mg, containing 4 mg, 0.04 mmol BnOH), the monomer (382 mg, 2 mmol), and 4 mL of toluene were added to an ampule bottom equipped with a magnetic stirrer. The ampule was placed in an oil bath at 100 °C. After 36 h, a portion of the solution was withdrawn to determine the conversion of the monomer by ^{1}H NMR. The polymer was isolated by precipitating the toluene solution into cold hexane, collecting the precipitate, and drying it under vacuum at 40 °C for 24 h. Other polymerization procedures were similar, except for differences in the feed ratio.

RESULTS AND DISCUSSION

Selection of Catalysts. The cleavage of asymmetric diesters at different acyl-oxygen bonds results in the formation of distinct polymer chain structures. Since the insertion of a monomer influences the two adjacent repeating units, we grouped three repeating units together to analyze the potential chain structures, as illustrated in Table S2. We first attempted the ROP of L-tBMG using Stannous octoate ($Sn(Oct)_2$) (Table 1, entry 1). Due to the lack of regioselectivity in $Sn(Oct)_2$, the arrangement of the two hydroxy acid units within the polymer chain was random (Figure S4). This result aligns with the ROP of *rac*-PDD monomers reported by Loos

https://doi.org/10.1021/acs.macromol.4c02286
Macromolecules 2024, 57, 11476−11487

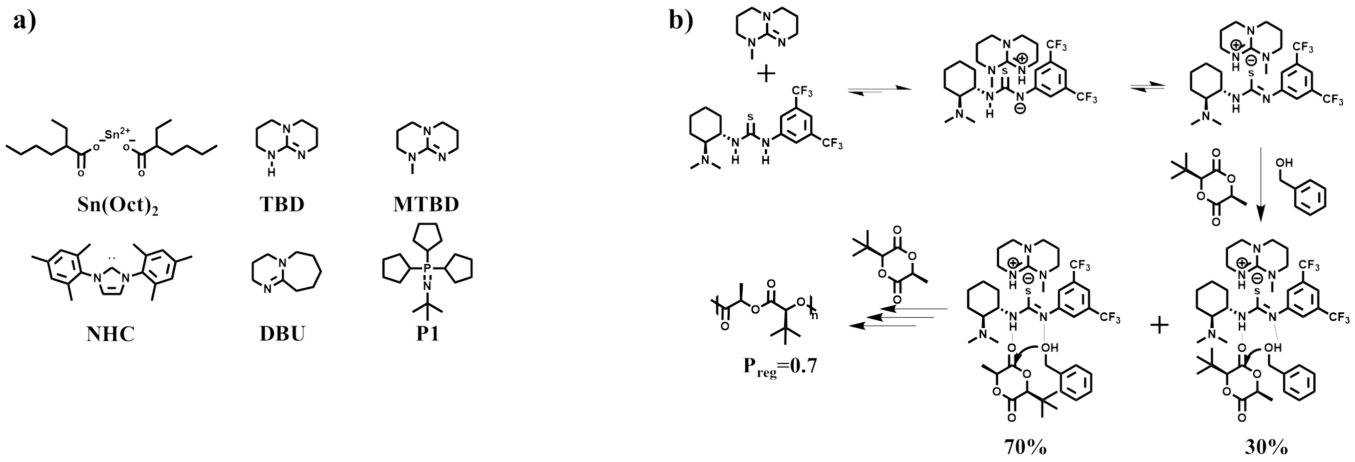

Figure 1. (a) Structural formulas of catalysts in Table 1. (b) Possible mechanism for the ROP of L-tBMG catalyzed by TU/MTBD.

Table 2. Polymerization Data of L-tBMG by Complexes[a]

entry	Cat	[M]/[C]/[I]	time (h)	Conv.[b] (%)	$M_{n\ theo}$[c] (kDa)	$M_{n\ GPC}$[d] (kDa)	$Đ$	chain regularity[e] (%)
1	SALC1	100/1/1	72					
2	SALC2	100/1/1	72					
3	SALC3	100/1/1	72					
4	SALC4	100/1/1	72	95	17.6	15.6	1.13	67
5	SALC5	100/1/1	72	92	17.1	15.3	1.12	70
6	SALC6	100/1/1	72	74	13.7	11.9	1.22	93[f]
7	$SALC7_R$	100/1/1	72	56	10.4	10.5	1.15	88
8	$SALC7_S$	100/1/1	72	71	13.2	11.0	1.20	70
9[g]	SIFC1	100/1/1	72					
10[g]	SIFC2	100/1/1	72					

[a]All polymerizations were carried out in 4 mL of tol [M] = 0.5 mol/L, the reaction temperature was 100 °C. [b]Measured by ^{1}H NMR. [c]Calculated from the equation molecular weight of L-tBMG × [M]/[I] × conversion. [d]Obtained by GPC in DMF against polystyrene standards. [e]Calculated from the equation chain regularity = (1 − regiodefect) × 100%. The regiodefect was determined by HSQC and HMBC, calculated by ^{1}H NMR. [f]Calculated by ^{1}H NMR and q-^{13}C NMR [g]Carried out in 2 mL of CHO solution [M] = 1 mol/L.

and co-workers.[48] An increase in the steric hindrance of the substituent can lead to a change in the catalyst's site of initiation, thereby resulting in regio-selectivity.[28,29,33,49] This may explain why $Sn(Oct)_2$ does not exhibit regioselectivity. To achieve alternating copolymers with high regularity, we introduced an organic base catalytic system for the ROP of L-tBMG.

We then attempted to catalyze the ROP of L-tBMG using various organic bases as catalysts (Figure 1a). The regioselectivity of 1,5,7-triazabicyclo[4.4.0]dec-5-ene (TBD) was 51%, while 7-methyl-1,5,7-triazabicyclo[4.4.0]dec-5-ene (MTBD) increased this to 57% (Table 1 entries 2 and 3) (Figure S5 and S6). The addition of a methyl group to the catalyst resulted in a significant improvement in selectivity compared to TBD. Therefore, increasing the steric hindrance of the substituent group can further enhance the catalyst's regioselectivity. The symmetrical distribution of two mesityl groups in the 1,3-dimesityl-1*H*-imidazol-3-ium-2-ide (NHC) structure makes it a promising candidate as a catalyst. Consequently, we attempted to use NHC to catalyze the ROP of L-tBMG. As expected, NHC achieved 53% chain regularity at a higher temperature (Table 1 entry 6) (Figure S9), compared to approximately 35% for MTBD and 25% for DBU (Figure S7 and S8).

We also observed that the selectivity of MTBD was 57% at 25 °C (Table 1 entry 3) (Figure S6) but decreased to 35% when the temperature was raised to 40 °C (Figure S7) (Table 1 entry 4). This observation suggests that temperature plays a significant role in influencing the regioselectivity of the catalyst in ROP, with lower temperatures favoring selective catalysis for MTBD.

Li et al. reported that a catalytic system composed of pyridine and urea exhibits excellent control in the ROP of lactones over a wide temperature range, attributed to the synergistic effect of pyridine and urea during catalysis.[50] When we applied this catalytic system to the ROP of L-tBMG, we observed that the catalytic systems of TBD, MTBD, and thiourea achieved selectivities of 58% (Figure S10) and 70% (Figure S11) after adding thiourea (Table 1 entries 2, 3, 7, and 8). Based on the study by Li and co-workers, we speculate that the involvement of thiourea increases the crowding around the catalytic active center (Figure 1b), making ROP of the ester bond on the sterically hindered side more difficult and enhancing selectivity. Despite achieving 70% chain regularity in the ROP of L-tBMG by optimizing the catalyst structure, polymerization temperature, and the interaction between the catalyst and cocatalyst, we did not obtain the ideal alternating copolymer structure of the two hydroxy acid units. Additionally, the racemization issue inherent in using organic bases as catalysts in ROP remains a drawback, preventing the formation of a completely isotactic molecular chain structure and a clear ^{1}H NMR spectrum.

To achieve an alternating copolymer structure of the two hydroxy acid units, such as poly(L-LA-*alt*-L-tBGA) (where L-

https://doi.org/10.1021/acs.macromol.4c02286
Macromolecules 2024, 57, 11476−11487

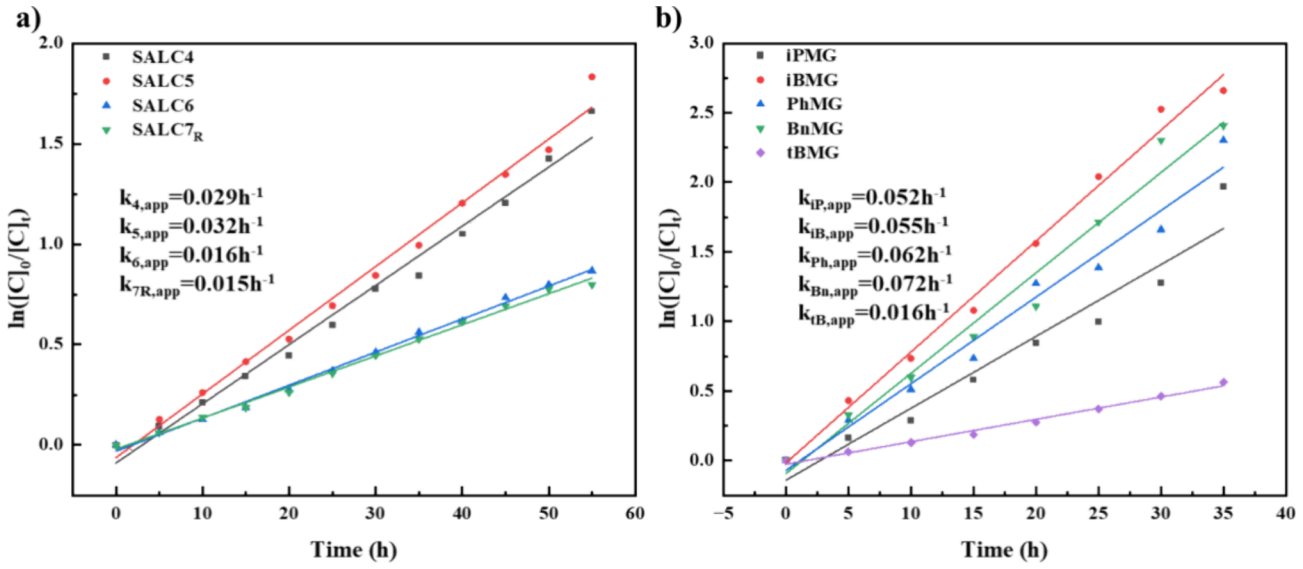

Figure 2. (a) ROP of L-tBMG with SALC4−7_R profiles of $\ln([C]_0/[C]_t)$ vs time. SALC4−7_R-catalyzed ROP of L-tBMG at [L-tBMG]/[BnOH]/[SALC] = 100:1:1 at 100 °C. (b) ROP of iPMG, iBMG, L-tBMG, PhMG, and BnMG with SALC6 profiles of $\ln([C]_0/[C]_t)$ vs time. SALC6-catalyzed ROP of asymmetric diesters at [M]/[BnOH]/[SALC6] = 100:1:1 at 100 °C.

LA is the lactic acid unit and L-tBGA is the substituted glycolic acid unit), a highly regioselective catalyst is required. Metal complexes, which offer the advantages of structural modifiability and the avoidance of monomer racemization during catalysis, have been used to catalyze the selective polymerization of esters with remarkable success.[29,49,51] Therefore, we investigated the catalytic performance of a variety of classical Schiff base complexes (Scheme 2) in the regioselective ROP of L-tBMG.

Initially, we used SALC1 to catalyze the ROP of L-tBMG at 100 °C. However, after 72 h, there was virtually no monomer conversion (Table 2 entry 1). Based on our previous research, we speculate that this may be due to the low activity of Schiff base complexes with this structure.[47] Consequently, we switched to using SALC2 and SALC3 as catalysts, which possess imine structures derived from propylene diamine and 2,2-dimethylpropane diamine. However, even after 72 h of polymerization at 100 °C, there was still virtually no conversion (Table 2 entries 2 and 3). This could be attributed to the strong steric hindrance of the *tert*-butyl group, which makes it difficult for the metal active center to coordinate with the ester during polymerization.

To verify this hypothesis, we tested SALC4 and SALC5, which have not stereo steric volume hindrance. After 72 h of polymerization at 100 °C, the conversion of the monomer was 94.7 and 92.1%, respectively (Table 2 entries 4 and 5). As shown in the Figure 2a, the ROP of L-tBMG catalyzed by SALC4 and SALC5 follows first-order kinetics, exhibiting the highest catalytic rates among all the Schiff base catalysts we tested($k_{4,app}$ = 0.029 h^{-1}, $k_{5,app}$ = 0.032 h^{-1}).These results indicate that the imine structures derived from propylene diamine and 2,2-dimethylpropane diamine can ensure sufficient ROP activity for Schiff base aluminum complexes, while the inability of SALC2 and SALC3 to catalyze ROP is due to the excessive steric hindrance of the *tert*-butyl group.

Although SALC4 and SALC5 already exhibited high activity, the chain regularity of the resulting polymers was not ideal, with a maximum of only 70% (Figure S16) (Table 2 entry 5). To obtain polymers with higher chain regularity, we attempt to increase the crowding around the metal active centers of the catalysts. However, the results using SALC2 and SALC3 as catalyst indicate that the *tert*-butyl substituents are too bulky to achieve effective ROP. Considering that electron-withdrawing groups on the benzene ring can enhance the catalytic activity of the metal center,[47] and that bulky groups on the benzene ring can improve the regio-selectivity of ROP for Schiff base complexes, we introduced chlorine atoms as substituents to increase the steric hindrance at the metal active center without losing catalytic activity. SALC6 was then used to catalyze the polymerization of L-tBMG at 100 °C. After 72 h, the conversion of monomer was 73.5% (Table 2 entry 6). Remarkably, the polymer chain regularity achieved with the SALC6 complex reached 93% (Figure S17, Figure 6e), resulting in almost completely alternating polymer structures.

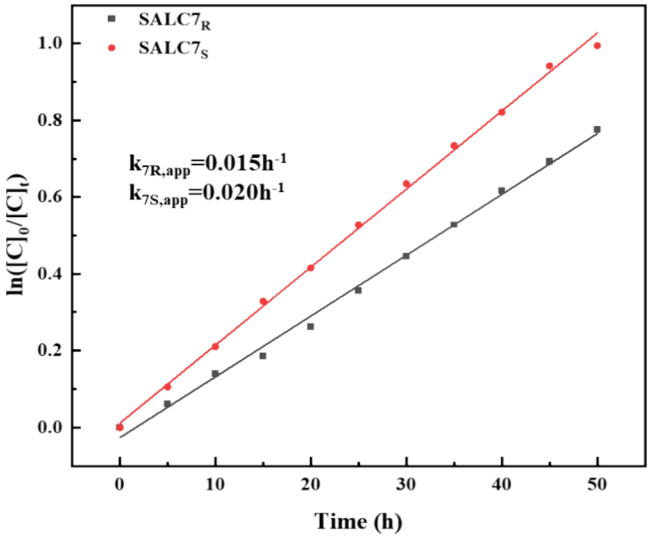

Figure 3. ROP of L-tBMG with SALC7_S,7_R profiles of $\ln([C]_0/[C]_t)$ vs time. SALC7_S,7_R-catalyzed ROP of L-tBMG at [L-tBMG]/[BnOH]/[SALC] = 100:1:1 at 100 °C.

https://doi.org/10.1021/acs.macromol.4c02286
Macromolecules 2024, 57, 11476−11487

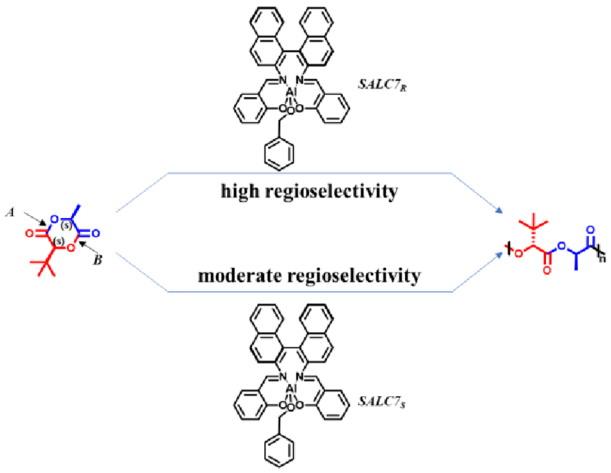

	A site		B site		k_{app}
	Charity match	Steric stereo volume	Charity match	Steric stereo volume	
$SALC7_R$	✖	✖	✖	○	$k_{7S,app}>k_{7R,app}$
$SALC7_S$	○	✖	○	○	
Regio-selectivity	$P_B>P_A$				

Figure 4. Ring-opening site determination. Circles represent which side of A or B is more dominant in ROP.

Coates and co-workers suggested that for Schiff base aluminum catalysts with a bridging moiety in the ligand structure of a binaphthalene group, the configuration of this bridge influences the chiral selectivity of the metal center. Specifically, when the bridging part is in the *R* configuration, the metal center preferentially coordinates with the D chiral center of the asymmetric diester, whereas in the *S* configuration, it favors coordination with the L chirality of the diester. Considering the proposed mechanism of regioselective ROP through chiral mismatch by Coates and co-workers,[29] we designed enantiomerically pure complexes with a binaphthyl framework, $SALC7_R$, $SALC7_S$ (Scheme 2). The $SALC7_R$, $SALC7_S$ was used to catalyze the polymerization of L-tBMG at 100 °C. After 72 h, the conversion of the monomer was 56% and 71%, respectively, respectively (Table 2 entries 7 and 8). However, the polymer catalyzed by $SALC7_R$ exhibited chain regularity of up to 88% (Figure S18) (Table 2 entry 7), consistent with Coates' study. Therefore, we speculate that our experimental results follow a similar mechanism to Coates' study. As shown in Figure 4, when using $SALC7_R$ to catalyze L-tBMG, the mismatch of chiral sites makes it difficult for $SALC7_R$ to coordinate effectively with L-tBMG. Additionally, the large size of the *tert*-butyl group of L-tBMG makes it more challenging for $SALC7_R$ to continue coordinating from the *tert*-butyl side under the premise of chiral mismatch. In contrast, when using $SALC7_S$ to catalyze L-tBMG, there is no chiral mismatch, and the *tert*-butyl group of L-tBMG is not sufficient to prevent the catalyst from coordinating from the *tert*-butyl side. Therefore, under the influence of these dual factors, $SALC7_R$ exhibits better selectivity for L-tBMG than $SALC7_S$. To test this hypothesis, we obtained kinetic plots for $SALC7_R$ and $SALC7_S$ by ^1H NMR. As shown in the Figure 3, the ROP of L-tBMG catalyzed by $SALC7_R$ and $SALC7_S$ follows first-order kinetics. Kinetic constants $k_{7R,app}$ (0.015 h^{-1}) is lower than $k_{7S,app}$ (0.020 h^{-1}), indicating that the mismatch of chiral sites limit the coordination of $SALC_{7R}$ with L-tBMG and the large *tert*-butyl group further limit the coordination of $SALC_{7R}$ and L-tBMG, thereby affecting catalyst activity. These findings support our hypothesis that high regioselectivity for the ROP of L-tBMG can be achieved through a chiral mismatch mechanism.

The above experimental results demonstrate that increasing steric hindrance at the catalytic active center and utilizing chiral mismatch can both achieve the desired regioselective ROP (Table 2 entries 6 and 7). Simultaneously, as shown in the kinetic experiments (Figure 2 and Figure 3), the ROP of L-tBMG catalyzed by SALC6 and $SALC7_R$ follows first-order kinetics, with both catalysts exhibiting similar activities($k_{6,app}$ = 0.016 h^{-1}, $k_{7R,app}$ = 0.015 h^{-1}).

Since SALC6 only triggers 70 monomers to participate in chain growth, this is not conducive for us to continue to explore other properties (e.g., mechanical properties) of the polymer in depth. We attempted to synthesize SALC8, intending to utilize the strong electron-withdrawal effect of the Br atom to further enhance the activity of the catalyst. But the polymerization involving SALC8 still yields polymers with a molecular chain regularity of about 92% (Figure S52, 53). Unfortunately, due to the large size of the Br atom, this catalyst can only catalyze 50 monomers for chain growth (Table S4). Because of the special chiral mismatch mechanism of SALC7, we wanted to know whether the polymerization system composed of monomers with different rotational strengths and the catalyst could result in a polymer structure with regionally regular but chiral blocks. Unfortunately, The

https://doi.org/10.1021/acs.macromol.4c02286
Macromolecules 2024, 57, 11476−11487

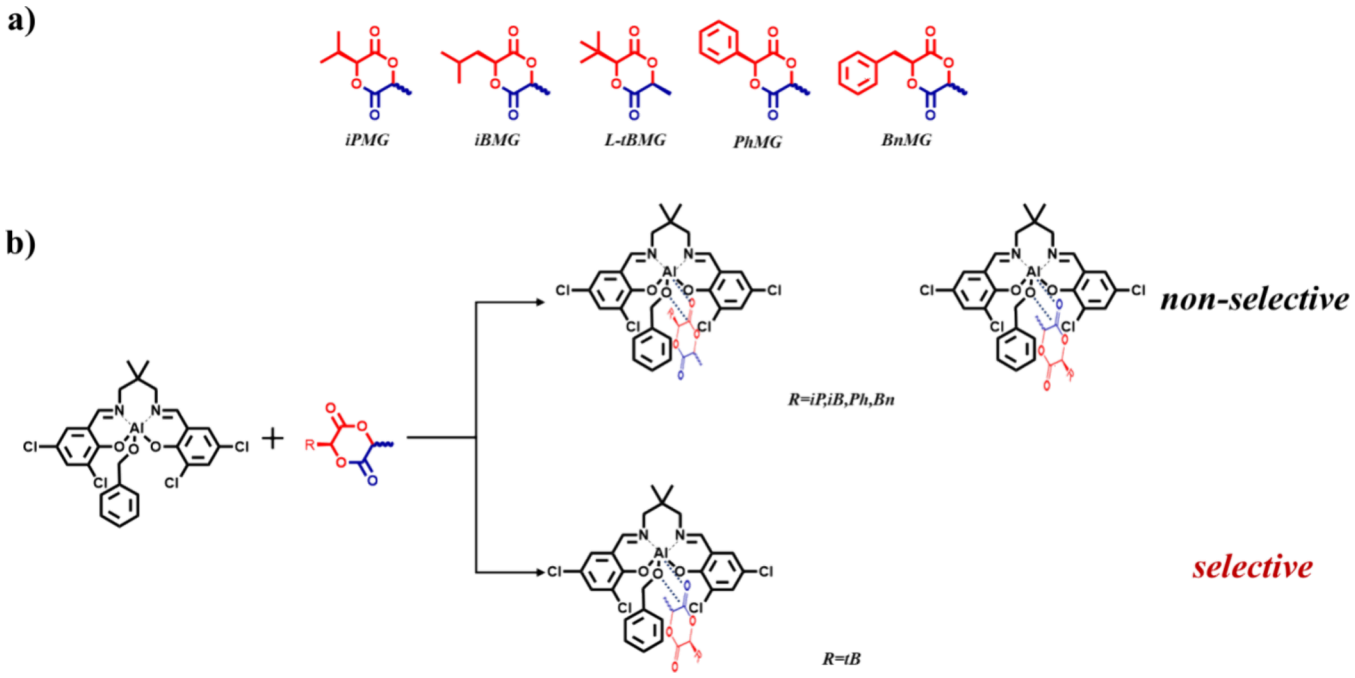

Figure 5. (a) Structural formulas of asymmetric diesters. (b) Relationship of the ring-opening site with substituent groups.

Table 3. Polymerization of Asymmetric Diesters with SALC6[a]

entry	monomer	[M]/[C]/[I]	time (h)	T (°C)	Conv.[b] (%)	$M_{n\ theo}$[c] (kDa)	$M_{n\ GPC}$[d] (kDa)	$Đ$
1	iPMG	100/1/1	72	100	94	16.1	16.9	1.12
2	iBMG	100/1/1	72	100	91	16.9	11.9	1.35
3	PhMG	100/1/1	72	100	90	18.4	17.2	1.32
4	BnMG	100/1/1	72	100	92	20.1	19.1	1.40

[a]All polymerizations were carried out in 4 mL of toluene, [M] = 0.5 mol/L. [b]Measured by ^{1}H NMR. [c]Calculated from the equation molecular weight of monomer × [M]/[I] × conversion. [d]Obtained by GPC in DMF against polystyrene standards.

Scheme 3. Repulsion between the Chain End and the Monomers

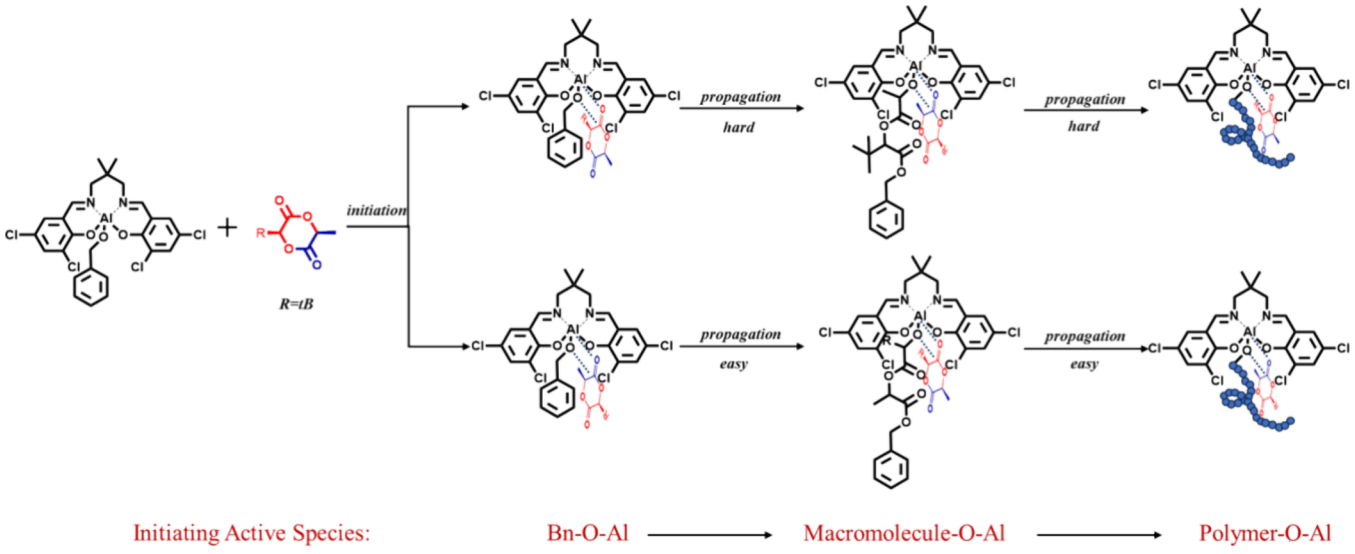

experimental results (Table S4) showed that no regular chain structure could be achieved in either reaction cast combination (L-tBMG with *rac*-SALC7, *rac*-tBMG with SALC7$_R$, *rac*-tBMG with SALC7$_S$). Effective peak attribution could not be performed based on the ^{1}H NMR spectra (Figures S49−S51).

Considering the stringent catalytic conditions required for Schiff base aluminum complexes, we attempted to use Schiff base iron complexes (SIFC) to catalyze the ROP of L-tBMG. We synthesized SIFC1 and SIFC2 and catalyzed the polymerization of L-tBMG at 100 °C for 24 h (Table 2 entries 9 and 10). Due to the strong Lewis acidity of SIFC,[43] we could

https://doi.org/10.1021/acs.macromol.4c02286
Macromolecules 2024, 57, 11476−11487

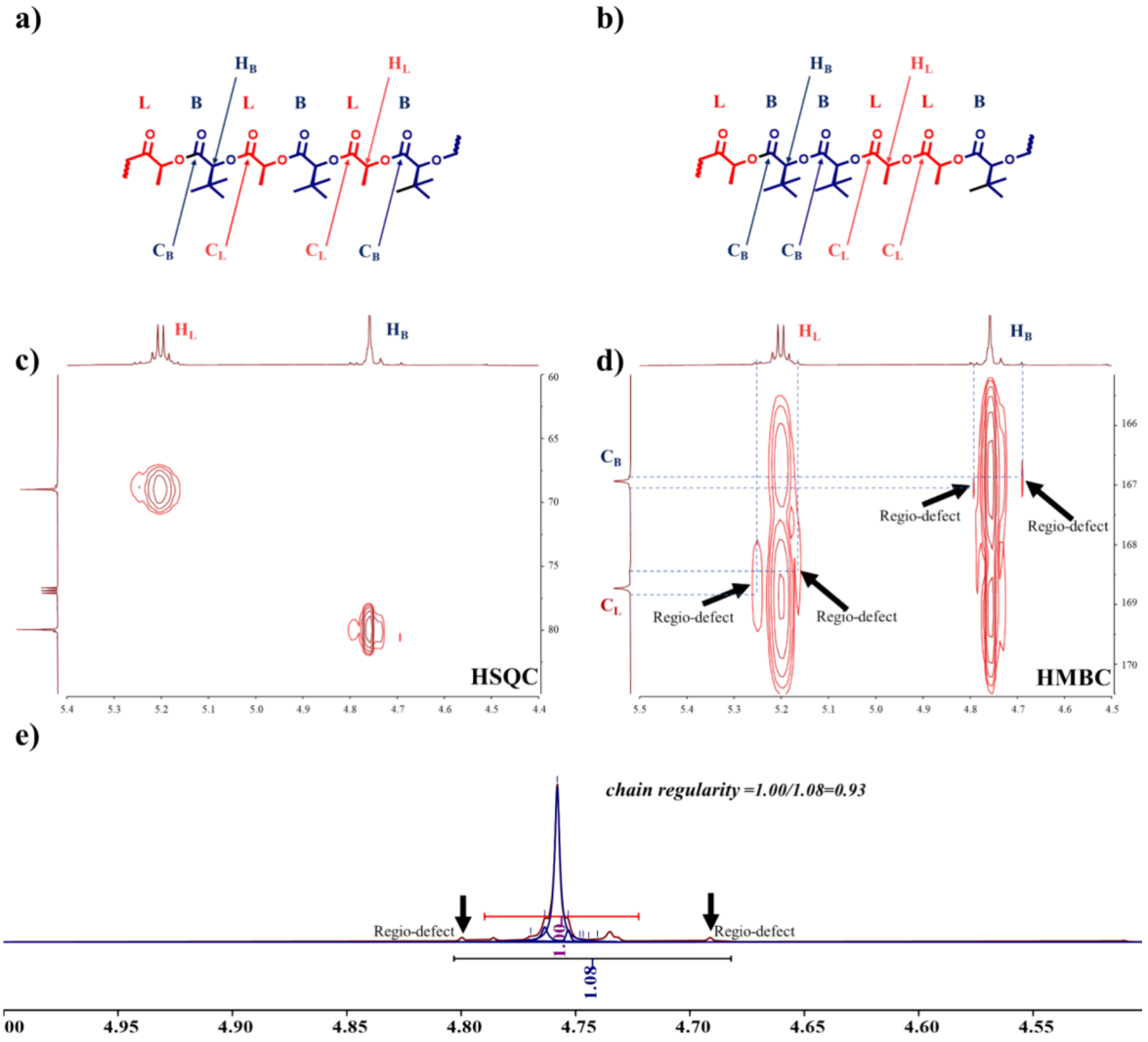

Figure 6. NMR spectra used for the chain regularity calculation. (a) Ideal structure of the polymer. (b) Polymer structure with regioselective defect. (c) HSQC and (d) HMBC spectra showing the methylene and carbonyl regions. (e) ^{1}H NMR spectrum of the methylene region.

only use oxidized cyclohexene as the solvent and initiator. But, the *tert*-butyl substituents are too bulky to achieve effective ROP.

Given the outstanding regioselectivity in the polymerization of L-tBMG using SALC6 as a catalyst, we sought to further investigate the mechanism of this catalyst in the regioselective polymerization of asymmetric diester. We attempted to use SALC6 to catalyze the ROP of iPMG, iBMG, PhMG, and BnMG (Figure 5a). As shown in Table 3, SALC6 did not exhibit ideal regioselectivity in the polymerization of these four monomers with different structure (Figures S20−S27).

We speculate that the regioselectivity of SALC6 is achieved through the stereo steric volume repulsion between its chlorine atom and the *tert*-butyl group of L-tBMG (Figure 5b). Due to the relatively large atomic radius of the chlorine atom and the significant volume of the *tert*-butyl substituent, the coordination of the carbonyl group on the *tert*-butyl side with the metal active center is more challenging compared to the carbonyl group on the methyl side, allowing only the ester bond on the methyl side to be activated. As chain growth proceeds (Scheme 3), the initiating active species gradually increase in size, growing from Bn−O-Al to macromolecule−O-Al. This leads to a more crowded active center, favoring the ring-opening of the ester group on the methyl side of the monomer. When the chain reaches a certain length, the active species grow from macromolecule−O-Al to polymer−O-Al. Due to the coiling of the polymer chains, the space around the active center becomes further compressed, which further restricts the ring-opening polymerization of the monomer on the *tert*-butyl side. Additionally, the electron-withdrawing effect of the chlorine atom ensures considerable activity, ultimately achieving highly efficient regioselective ROP.

When the steric volume of the substituent changes slightly, the volume repulsion may be insufficient to maintain the exclusive coordination of the carbonyl group on the methyl side with the metal active center. As shown in the Figure 5b, Isopropyl, isobutyl, phenyl, and benzyl groups can rotate through the C−C bond to obtain a suitable conformation, allowing the carbonyl group on the bulky substituent side to coordinate with the metal active center. However, due to differences in the rotatable angles of the carbon−carbon bonds in different substituents, the probability of forming a conformation suitable for ROP on the bulky substituent side varies. For example, in iPMG, the β carbon atom has two methyl groups, while in iBMG, the γ carbon atom has two methyl groups. The two methyl groups in iBMG are farther

https://doi.org/10.1021/acs.macromol.4c02286
Macromolecules 2024, 57, 11476−11487

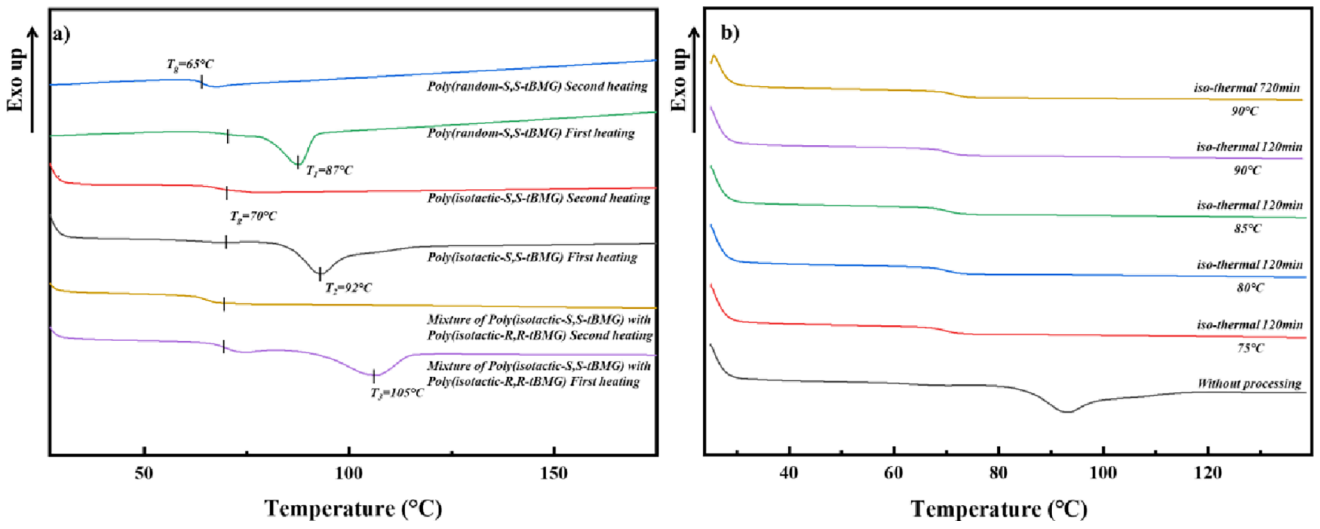

Figure 7. (a) Differential scanning calorimetry (DSC) curves of poly(random-S,S-tBMG), poly(isotactic-S,S-tBMG), and mixture of poly(isotactic-S,S-tBMG) with poly(isotactic-R,R-tBMG). (b) Isothermal crystallization curves of poly(isotactic-S,S-tBMG) under different temperatures.

from the carbonyl group, providing more space for rotation, leading to a higher probability of forming a conformation suitable for ROP on the bulky substituent side than in iPMG. Similarly, PhMG has a phenyl group on the α-carbon atom, while BnMG has a phenyl group on the β-carbon atom. The phenyl group in BnMG is farther from the carbonyl group, offering more rotational space, which increases the likelihood of forming a conformation suitable for ROP on the bulky substituent side compared to PhMG. However, the β-carbon atom of L-tBMG is substituted by three methyl groups, making it almost impossible to achieve a conformation favorable for ROP on the bulky substituent side through free rotation of the C−C bond. We verified this hypothesis through kinetic experiments. As shown in the Figure 2b, the ROP of the five asymmetric esters catalyzed by SALC6 follow first-order kinetics. Additionally, the variation in the order kinetic constant aligns with our conformational analysis for different asymmetric diesters ($k_{iP,app}$(0.052 h^{-1})< $k_{iB,app}$(0.055 h^{-1}), $k_{Ph,app}$(0.062 h^{-1})<$k_{Bn,app}$(0.072 h^{-1}), $k_{tB,app}$ = 0.016 h^{-1}).

Meanwhile, according to Table S3, the melting point differences between different components of the other four asymmetric cross esters are too small to satisfy the technical requirements for melt crystallization. Therefore, we do not have a suitable method to obtain monomers with high optical purity to further discuss the ROP of the other diesters catalyzed by SALC7$_R$.This part of the work still needs to be further investigated in the next work.

Characterization of the Molecular Chain Structure. To better understand the sequence structure of the polymer and quantitatively determine the chain regularity, we employed a combination of H nuclear magnetic resonance (^{1}H NMR), quantitative nuclear magnetic resonance carbon spectroscopy (q-^{13}C NMR), heteronuclear singular quantum correlation (HSQC), and heteronuclear multiple bond correlation (HMBC) to analyze the polymer chain structure in detail. HSQC provides coupling information for carbon atoms directly bonded to hydrogen atoms, while HMBC provides coupling information for carbon atoms within three single bonds of hydrogen atoms.

As shown in Figure 6c, the quartet at 5.20 ppm and the singlet at 4.76 ppm correspond to two carbon atoms directly bonded at 69.00 and 80.00 ppm, respectively. We define the hydrogen atom at 5.20 ppm as H_L (i.e., C−H from the lactic acid unit) and the hydrogen atom at 4.76 ppm as H_B (i.e., C−H from 2-*tert*-butylglycolic acid). We designate the carbon atom at 166.93 ppm as C_B (i.e., the carbonyl carbon from 2-*tert*-butylglycolic acid) and the carbon atom at 168.73 ppm as C_L (i.e., the carbonyl carbon from lactic acid).

If we assume the polymer chain is a perfectly alternating sequence, then each H_L in the HMBC coupling range will couple with one C_B and one C_L, and each H_B will also couple with one C_B and one C_L (Figure 6a). If there are defects in the molecular chain, H_L will couple with two C_L, and H_B will couple with two C_B (Figure 6b). Thus, using the HMBC spectrum, we can identify peaks corresponding to regio defects (Figure 6d). In the HMBC spectrum, the red contour in the center of the plot represents the coupling of hydrogen and carbon atoms at the corresponding horizontal and vertical coordinates. According to Figure 6d, peaks at 4.69 and 4.79 ppm correspond to the H_B which couple with two C_B, indicating there are regio-defect peaks. Similarly, peaks at 5.16 and 5.25 ppm correspond to the H_L coupling with two C_L, also identifying them as regio-defect peaks. The peak at 4.76 ppm is formed by L-tBMG after the polymer chain is inserted by breaking on the acyl-oxygen bond side of the lactate unit. Since the optical purity of L-tBMG is 99.11%, the small peak around 4.76 ppm is formed by tBMG with different optical rotations after the polymer chain is inserted by breaking on the acyl-oxygen bond side of the lactate unit.

Due to the overlap of the quartet at 5.20 ppm, we chose to integrate the clearer singlet at 4.76 ppm. Based on the integration area ratio, the chain regularity was determined to be 93% (Figure 6e). We also determined the integral intensity of the carbonyl carbon using q-^{13}C NMR. The ratio of the integral intensities (Figure S17) indicates a molecular chain regularity of 94%. Considering potential errors, the results obtained using both q-^{13}C NMR and ^{1}H NMR are reliable.

Thermal Properties of Copolymers. To examine the effect of molecular chain regularity on the thermal properties of the copolymers, we analyzed the thermal properties using differential scanning calorimetry (DSC) (Figure 7a). The T_g of the atactic PtBMG (12.3 kg/mol, $Đ$ = 1.36) synthesized using $Sn(Oct)_2$ as the catalyst and benzyl alcohol as the initiator at 180 °C showed a T_g at 65 °C. The T_g of the isotactic PtBMG

https://doi.org/10.1021/acs.macromol.4c02286
Macromolecules 2024, 57, 11476−11487

(11.9 kg/mol, $Đ$ = 1.22) prepared using the SALC6 as the catalyst and BnOH as the initiator at 100 °C, was 70 °C. This suggests that the T_g of these polymers can increase with greater molecular chain regularity when the molecular weights are similar.[28,33,49] Studies have shown that as the molecular chain regularity increases, some polymers can transition from amorphous to crystalline. For example, Wu et al. obtained polymers with regular molecular chains by catalyzing the ROP of MPDD with TMP-Zn, exhibiting crystallinity distinct from atactic polymers, with two melting points, 129.3 and 152.4 °C.[28] We conducted isothermal crystallization experiments on the polymers using DSC at five different crystallization temperatures (Figure 7b). Unfortunately, even with a molecular chain regularity of 93%, The copolymer still exhibited no melting point. This result contrasts with Wu et al.'s and Coates et al.'s, Arakawa et al.'s study.[29,52] Considering that this result might be caused by too short isothermal crystallization time, we tried to perform longer isothermal crystallization experiments. Unfortunately, the polymers remained amorphous (Figure 7,Figure S55) after a longer isothermal crystallization experiments. Considering that the blending of polymers of opposite chirality might be able to form cubic complex crystals, we polymerized to obtain Poly(R,R-tBMG) (chain regularity = 0.93, 12.1 kg/mol, $Đ$ = 1.25, Table S4, Figure S54). The experimental results shown in Figure 7 indicate that the blends of the polymers of opposite chirality are still amorphous, although there is a large increase in T_3 compared to T_1 and T_2 during the first warming process, which suggests that perhaps this regular polymer is capable of crystallization, only that this condition needs to be further explored.

CONCLUSIONS

In this study, we investigated the catalytic performance of various Schiff base complexes in the regioselective ROP of L-tBMG and developed a new application for Schiff base aluminum complexes in the regioselective polymerization of asymmetric diesters. Our findings demonstrate that effective regioselective ROP can be achieved by rationally adjusting the structure of the Schiff base-aluminum complex. This selectivity can be realized through two mechanisms: one relying on the steric repulsion between the substituents of the SALC and the monomer, and the other on the chiral mismatch between the asymmetric diester and the bridged moiety of the catalyst.

Furthermore, we found that changes in the substituent volume of the monomer can induce conformational variations through C−C rotation, affecting the probability of coordination of the Schiff base aluminum on both sides of the asymmetric diester. This sensitivity to monomer substituent volume makes the first mechanism particularly responsive to such changes. In the present work, we synthesized nearly perfectly alternating copolymers of L-tBGA and LA, with chain regularity values reaching up to 0.93, utilizing steric repulsion between Schiff base aluminum and L-tBMG. DSC experiments revealed that the thermal properties of the copolyesters can be modulated by the sequence structure of the two monomer units. The random 1:1 copolymer of L-tBGA and LA exhibited a T_g of 65 °C, while the copolymer with a chain regularity value of 0.93 had a T_g of 70 °C.

ASSOCIATED CONTENT

Supporting Information

The Supporting Information is available free of charge at https://pubs.acs.org/doi/10.1021/acs.macromol.4c02286.

Materials, synthesis of monomers, purification of (3*S*,6*S*)-3-*tert*-butyl-6-methyl-1,4-dioxane-2,5-dione, characterization of the polymer chain structure, ^{1}H NMR of ligands and complexes, Ms of complexes, chiral gas chromatography of the other asymmetric diesters, and DSC experiment (PDF)

AUTHOR INFORMATION

Corresponding Authors

Ranlong Duan − *Key Laboratory of Polymer Ecomaterials, Changchun Institute of Applied Chemistry, Chinese Academy of Sciences, Changchun 130022, P. R. China;* orcid.org/0009-0004-3259-6280; Email: duanranlong@ciac.ac.cn

Xinchao Bian − *Key Laboratory of Polymer Ecomaterials, Changchun Institute of Applied Chemistry, Chinese Academy of Sciences, Changchun 130022, P. R. China; School of Applied Chemistry and Engineering, University of Science and Technology of China, Hefei 230026, P. R. China;* orcid.org/0000-0003-2787-1503; Email: xcbian@ciac.ac.cn

Authors

Yeqi Du − *Key Laboratory of Polymer Ecomaterials, Changchun Institute of Applied Chemistry, Chinese Academy of Sciences, Changchun 130022, P. R. China; School of Applied Chemistry and Engineering, University of Science and Technology of China, Hefei 230026, P. R. China*

Jinbo Hu − *Key Laboratory of Polymer Ecomaterials, Changchun Institute of Applied Chemistry, Chinese Academy of Sciences, Changchun 130022, P. R. China; School of Applied Chemistry and Engineering, University of Science and Technology of China, Hefei 230026, P. R. China*

Wenbo Wang − *Key Laboratory of Polymer Ecomaterials, Changchun Institute of Applied Chemistry, Chinese Academy of Sciences, Changchun 130022, P. R. China; School of Applied Chemistry and Engineering, University of Science and Technology of China, Hefei 230026, P. R. China*

Xinyan Liu − *Key Laboratory of Polymer Ecomaterials, Changchun Institute of Applied Chemistry, Chinese Academy of Sciences, Changchun 130022, P. R. China; School of Applied Chemistry and Engineering, University of Science and Technology of China, Hefei 230026, P. R. China*

Yanlong Liu − *Key Laboratory of Polymer Ecomaterials, Changchun Institute of Applied Chemistry, Chinese Academy of Sciences, Changchun 130022, P. R. China; School of Applied Chemistry and Engineering, University of Science and Technology of China, Hefei 230026, P. R. China*

Xuesi Chen − *Key Laboratory of Polymer Ecomaterials, Changchun Institute of Applied Chemistry, Chinese Academy of Sciences, Changchun 130022, P. R. China; School of Applied Chemistry and Engineering, University of Science and Technology of China, Hefei 230026, P. R. China;* orcid.org/0000-0003-3542-9256

Complete contact information is available at: https://pubs.acs.org/10.1021/acs.macromol.4c02286

Notes

The authors declare no competing financial interest.

https://doi.org/10.1021/acs.macromol.4c02286
Macromolecules 2024, 57, 11476−11487

■ ACKNOWLEDGMENTS

This study was supported by the National Key Research and Development Program of China (no. 2021YFD1700700).

■ REFERENCES

(1) Rochman, C. M.; Browne, M. A.; Halpern, B. S.; Hentschel, B. T.; Hoh, E.; Karapanagioti, H. K.; Rios-Mendoza, L. M.; Takada, H.; Teh, S.; Thompson, R. C. Classify plastic waste as hazardous. *Nature* **2013**, *494* (7436), 169−171.
(2) Napper, I.; Thompson, R. Plastics and the Environment. *Annual Review of Environment and Resources* **2023**, *48* (1), 55−79.
(3) Brandon, A.; Vanapalli, K. R.; Martin, O. V.; Dijkstra, H.; De la Torre, G. E.; Hartmann, N. B.; Meier, M. A. R.; Pathak, G.; Busch, P.-O.; Ma, D.; Iacovido, D.; Birkbeck, C. D.; Pacini, H. Charting success for the Plastics Treaty. *One Earth* **2023**, *6* (6), 575−581.
(4) Gandini, A.; Lacerda, T. M.; Carvalho, A. J.; Trovatti, E. Progress of polymers from renewable resources: furans, vegetable oils, and polysaccharides. *Chem. Rev.* **2016**, *116* (3), 1637−1669.
(5) Vilela, C.; Sousa, A. F.; Fonseca, A. C.; Serra, A. C.; Coelho, J. F.; Freire, C. S.; Silvestre, A. J. The quest for sustainable polyesters−insights into the future. *Polym. Chem.* **2014**, *5* (9), 3119−3141.
(6) Miller, S. A. Sustainable polymers: replacing polymers derived from fossil fuels. *Polym. Chem.* **2014**, *5* (9), 3117−3118.
(7) Hillmyer, M. A.; Tolman, W. B. Aliphatic polyester block polymers: renewable, degradable, and sustainable. *Accounts of chemical research* **2014**, *47* (8), 2390−2396.
(8) Rajvanshi, J.; Sogani, M.; Kumar, A.; Arora, S.; Syed, Z.; Sonu, K.; Gupta, N. S.; Kalra, A. Perceiving biobased plastics as an alternative and innovative solution to combat plastic pollution for a circular economy. *Science of The Total Environment* **2023**, *874*, No. 162441.
(9) Dhaini, A.; Hardouin-Duparc, V.; Alaaeddine, A.; Carpentier, J.-F.; Guillaume, S. M. Recent advances in polyhydroxyalkanoates degradation and chemical recycling. *Prog. Polym. Sci.* **2024**, *149*, No. 101781.
(10) Nampoothiri, K. M.; Nair, N. R.; John, R. P. An overview of the recent developments in polylactide (PLA) research. *Bioresour. Technol.* **2010**, *101* (22), 8493−8501.
(11) Chen, G.-Q.; Patel, M. K. Plastics derived from biological sources: present and future: a technical and environmental review. *Chem. Rev.* **2012**, *112* (4), 2082−2099.
(12) Lutz, J.-F.; Ouchi, M.; Liu, D. R.; Sawamoto, M. Sequence-controlled polymers. *Science* **2013**, *341* (6146), No. 1238149.
(13) Badi, N.; Lutz, J.-F. Sequence control in polymer synthesis. *Chem. Soc. Rev.* **2009**, *38* (12), 3383−3390.
(14) Matyjaszewski, K. Architecturally complex polymers with controlled heterogeneity. *Science* **2011**, *333* (6046), 1104−1105.
(15) Swisher, J. H.; Nowalk, J. A.; Washington, M. A.; Meyer, T. Y. Properties and Applications of Sequence-Controlled Polymers. *Sequence-Controlled Polymers* **2018**, 435−478.
(16) Jaffredo, C. G.; Chapurina, Y.; Guillaume, S. M.; Carpentier, J. F. From syndiotactic homopolymers to chemically tunable alternating copolymers: Highly active Yttrium complexes for stereoselective ring-opening polymerization of *β*-Malolactonates. *Angew. Chem., Int. Ed.* **2014**, *53* (10), 2687−2691.
(17) Nowalk, J. A.; Swisher, J. H.; Meyer, T. Y. Consequences of isolated critical monomer sequence errors for the hydrolysis behaviors of sequenced degradable polyesters. *Polym. Chem.* **2019**, *10* (36), 4930−4934.
(18) Li, J.; Stayshich, R. M.; Meyer, T. Y. Exploiting sequence to control the hydrolysis behavior of biodegradable PLGA copolymers. *J. Am. Chem. Soc.* **2011**, *133* (18), 6910−6913.
(19) Li, J.; Rothstein, S. N.; Little, S. R.; Edenborn, H. M.; Meyer, T. Y. The effect of monomer order on the hydrolysis of biodegradable poly (lactic-co-glycolic acid) repeating sequence copolymers. *J. Am. Chem. Soc.* **2012**, *134* (39), 16352−16359.
(20) Washington, M. A.; Balmert, S. C.; Fedorchak, M. V.; Little, S. R.; Watkins, S. C.; Meyer, T. Y. Monomer sequence in PLGA microparticles: Effects on acidic microclimates and in vivo inflammatory response. *Acta Biomaterialia* **2018**, *65*, 259−271.
(21) Washington, M. A.; Swiner, D. J.; Bell, K. R.; Fedorchak, M. V.; Little, S. R.; Meyer, T. Y. The impact of monomer sequence and stereochemistry on the swelling and erosion of biodegradable poly (lactic-co-glycolic acid) matrices. *Biomaterials* **2017**, *117*, 66−76.
(22) Longo, J. M.; Sanford, M. J.; Coates, G. W. Ring-opening copolymerization of epoxides and cyclic anhydrides with discrete metal complexes: structure−property relationships. *Chem. Rev.* **2016**, *116* (24), 15167−15197.
(23) Fieser, M. E.; Sanford, M. J.; Mitchell, L. A.; Dunbar, C. R.; Mandal, M.; Van Zee, N. J.; Urness, D. M.; Cramer, C. J.; Coates, G. W.; Tolman, W. B. Mechanistic insights into the alternating copolymerization of epoxides and cyclic anhydrides using a (Salph) AlCl and iminium salt catalytic system. *J. Am. Chem. Soc.* **2017**, *139* (42), 15222−15231.
(24) Lidston, C. A.; Abel, B. A.; Coates, G. W. Bifunctional catalysis prevents inhibition in reversible-deactivation ring-opening copolymerizations of epoxides and cyclic anhydrides. *J. Am. Chem. Soc.* **2020**, *142* (47), 20161−20169.
(25) Li, J.; Liu, Y.; Ren, W.-M.; Lu, X.-B. Enantioselective terpolymerization of racemic and meso-epoxides with anhydrides for preparation of chiral polyesters. *Proc. Natl. Acad. Sci. U. S. A.* **2020**, *117* (27), 15429−15436.
(26) Yi, N.; Chen, T. T.; Unruangsri, J.; Zhu, Y.; Williams, C. K. Orthogonal functionalization of alternating polyesters: selective patterning of (AB) n sequences. *Chemical Science* **2019**, *10* (43), 9974−9980.
(27) Li, H.; Zhao, J.; Zhang, G. Self-buffering organocatalysis tailoring alternating polyester. *ACS Macro Lett.* **2017**, *6* (10), 1094−1098.
(28) Jia, Z.; Jiang, J.; Zhang, X.; Cui, Y.; Chen, Z.; Pan, X.; Wu, J. Isotactic-alternating, heterotactic-alternating, and ABAA-type sequence-controlled copolyester syntheses via highly stereoselective and regioselective ring-opening polymerization of cyclic diesters. *J. Am. Chem. Soc.* **2021**, *143* (11), 4421−4432.
(29) Lu, Y.; Swisher, J. H.; Meyer, T. Y.; Coates, G. W. Chirality-directed regioselectivity: an approach for the synthesis of alternating poly (lactic-co-glycolic acid). *J. Am. Chem. Soc.* **2021**, *143* (11), 4119−4124.
(30) Zhu, Y.; Tao, Y. Stereoselective Ring-opening Polymerization of S-Carboxyanhydrides Using Salen Aluminum Catalysts: A Route to High-Isotactic Functionalized Polythioesters. *Angew. Chem., Int. Ed.* **2024**, *63* (9), No. e202317305.
(31) Takojima, K.; Makino, H.; Saito, T.; Yamamoto, T.; Tajima, K.; Isono, T.; Satoh, T. An organocatalytic ring-opening polymerization approach to highly alternating copolymers of lactic acid and glycolic acid. *Polymer chemistry* **2020**, *11* (39), 6365−6373.
(32) Kim, H. J.; Reddi, Y.; Cramer, C. J.; Hillmyer, M. A.; Ellison, C. J. Readily degradable aromatic polyesters from salicylic acid. *ACS Macro Lett.* **2020**, *9* (1), 96−102.
(33) Wang, Y.; Jia, Z.; Jiang, J.; Mao, X.; Pan, X.; Wu, J. Highly Regioselective Ring-Opening Polymerization of Cyclic Diester for Alternating Sequence-Controlled Copolymer Synthesis of Mandelic Acid and Glycolic Acid. *Macromolecules* **2019**, *52* (20), 7564−7571.
(34) Uhrich, K. E.; Cannizzaro, S. M.; Langer, R. S.; Shakesheff, K. M. Polymeric systems for controlled drug release. *Chem. Rev.* **1999**, *99* (11), 3181−3198.
(35) Terada, S.; Sato, M.; Sevy, A.; Vacanti, J. P. Tissue engineering in the twenty-first century. *Yonsei Medical Journal* **2000**, *41* (6), 685−691.
(36) Stanford, M. J.; Dove, A. P. Stereocontrolled ring-opening polymerisation of lactide. *Chem. Soc. Rev.* **2010**, *39* (2), 486−494.
(37) Ovitt, T. M.; Coates, G. W. Stereochemistry of lactide polymerization with chiral catalysts: new opportunities for stereocontrol using polymer exchange mechanisms. *J. Am. Chem. Soc.* **2002**, *124* (7), 1316−1326.
(38) Chile, L.-E.; Mehrkhodavandi, P.; Hatzikiriakos, S. G. A comparison of the rheological and mechanical properties of isotactic,

syndiotactic, and heterotactic poly (lactide). *Macromolecules* **2016**, *49* (3), 909−919.
(39) Anderson, K. S.; Schreck, K. M.; Hillmyer, M. A. Toughening polylactide. *Polym. Rev.* **2008**, *48* (1), 85−108.
(40) Tsuji, H. Poly (lactide) stereocomplexes: formation, structure, properties, degradation, and applications. *Macromol. Biosci.* **2005**, *5* (7), 569−597.
(41) Fukushima, K.; Kimura, Y. Stereocomplexed polylactides (Neo-PLA) as high-performance bio-based polymers: their formation, properties, and application. *Polym. Int.* **2006**, *55* (6), 626−642.
(42) Baker, G. L.; Vogel, E. B.; Smith, M. R., III Glass transitions in polylactides. *Polym. Rev.* **2008**, *48* (1), 64−84.
(43) Duan, R.; Hu, C.; Li, X.; Pang, X.; Sun, Z.; Chen, X.; Wang, X. Air-stable salen−iron complexes: Stereoselective catalysts for lactide and ε-caprolactone polymerization through in situ initiation. *Macromolecules* **2017**, *50* (23), 9188−9195.
(44) Nishioka, K.; Goto, H.; Sugimoto, H. Dual catalyst system for asymmetric alternating copolymerization of carbon dioxide and cyclohexene oxide with chiral aluminum complexes: Lewis base as catalyst activator and Lewis acid as monomer activator. *Macromolecules* **2012**, *45* (20), 8172−8192.
(45) Spassky, N.; Wisniewski, M.; Pluta, C.; Le Borgne, A. Highly stereoelective polymerization of rac-(D, L)-lactide with a chiral schiff's base/aluminium alkoxide initiator. *Macromol. Chem. Phys.* **1996**, *197* (9), 2627−2637.
(46) Duxbury, J. P.; Warne, J. N.; Mushtaq, R.; Ward, C.; Thornton-Pett, M.; Jiang, M.; Greatrex, R.; Kee, T. P. Phospho-aldol catalysis via chiral schiff base complexes of aluminum. *Organometallics* **2000**, *19* (22), 4445−4457.
(47) Du, H.; Pang, X.; Yu, H.; Zhuang, X.; Chen, X.; Cui, D.; Wang, X.; Jing, X. Polymerization of rac-lactide using Schiff base aluminum catalysts: structure, activity, and stereoselectivity. *Macromolecules* **2007**, *40* (6), 1904−1913.
(48) Nakajima, H.; Loos, K.; Ishizu, S.; Kimura, Y. Ring-Opening Polymerization of a New Diester Cyclic Dimer of Mandelic and Glycolic Acid: An Efficient Synthesis Method for Derivatives of Amorphous Polyglycolide with High Tg. *Macromol. Rapid Commun.* **2018**, *39* (12), No. 1700865.
(49) Lu, Y.; Coates, G. W. Pairing-Enhanced Regioselectivity: Synthesis of Alternating Poly (lactic-co-glycolic acid) from Racemic Methyl-Glycolide. *J. Am. Chem. Soc.* **2023**, *145* (41), 22425−22432.
(50) Feng, R.; Jie, S.; Braunstein, P.; Li, B.-G. Pyridyl-urea catalysts for the solvent-free ring-opening polymerization of lactones and trimethylene carbonate. *Eur. Polym. J.* **2019**, *121*, No. 109293.
(51) Zhong, Z.; Dijkstra, P. J.; Feijen, J. Controlled and stereoselective polymerization of lactide: Kinetics, selectivity, and microstructures. *J. Am. Chem. Soc.* **2003**, *125* (37), 11291−11298.
(52) Tsuji, H.; Yamasaki, M.; Arakawa, Y. Stereocomplex formation between enantiomeric alternating lactic acid-based copolymers as a versatile method for the preparation of high performance biobased biodegradable materials. *ACS Applied Polymer Materials* **2019**, *1* (6), 1476−1484.

https://doi.org/10.1021/acs.macromol.4c02286
Macromolecules 2024, 57, 11476−11487